# Monte Carlo simulation of electron swarms at low reduced electric fields

M. Yousfi, A. Hennad, and A. Alkaa
*Université Paul Sabatier, Centre de Physique Atomique, 118, Route de Narbonne, 31 062 Toulouse Cedex, France*
(Received 2 August 1993)

A Monte Carlo method, based on the classical null collision technique, is developed and applied for electron swarm simulation in weakly ionized gases at low $E/N$ values ($E$ being the electric field and $N$ the background gas density). The dominant low energy collisional processes (elastic, inelastic, and superelastic collisions) are properly considered. The influence of the thermal motion of background gas (target not assumed at rest) on electron kinetics, which can play an important role at very low $E/N$, is also taken into account. At zero field and low $E/N$ conditions, the influence of low energy collision processes on space and time evolution of electron swarm parameters is emphasized in atomic (He) and molecular ($H_2O$) gases. Then, the present Monte Carlo method is adapted to the low $E/N$ cases in strongly electronegative gases such as $SF_6$ to overcome the problem of the vanishing of seed electrons by attachment processes which can stop the simulation. In that case, an additional fictitious ionization process with constant collision frequency is considered to obtain hydrodynamic electron swarm parameters in $SF_6$ at low $E/N$.

PACS number(s): 52.20.Fs, 51.50.+v

## I. INTRODUCTION

Swarm characteristics (distribution functions and transport coefficients) of electrons moving in a weakly or partially ionized gas under the influence of an accelerating electric field can be numerically obtained either from the direct Boltzmann equation solution or from Monte Carlo simulation. Solution of the Boltzmann equation in a nonhydrodynamic regime involving time and in particular space variation of distribution functions constitutes a numerical challenge, while the Monte Carlo method is easier to develop in hydrodynamic as well as nonhydrodynamic regimes. However, the well known Monte Carlo drawback concerns the prohibitive computing time. But, due to progress in computer technology, calculation time is less and less a constraint. Monte Carlo methods can thus be considered as well adapted for numerical simulations of electron swarm motion in gas discharges whatever the geometry (one, two, or three dimensions), the regime (transient or steady, homogeneous or not), and the applied electric field. Concerning the applied electric field $E/N$ ($N$ being the gas density), there are some specific problems in Monte Carlo simulation which depend, in particular, on $E/N$ magnitude.

At high $E/N$ values, the large electron amplification due to ionizing collisions obviously enhances the number of electrons treated with Monte Carlo method and can considerably increase computing time. Such a problem—not emphasized in this paper—could be solved by using appropriate weighting techniques.

At low $E/N$ values, in the case of electron-molecule collisions, the first problem concerns the correct treatment of collision kinematics. This must include the motion of projectile electrons as well as the thermal motion of target molecules. The motion consideration of both projectile and target particles is important for low impact energy, i.e., at low $E/N$ values when energies of impinging electrons and target molecules are practically of the same order of magnitude. This is what happens at low electron energy not only during elastic collisions but also during inelastic and superelastic collisions involving rotational and vibrational energy levels of target molecule. For these cases, the correct treatment of the collision kinematics (i.e., without assuming molecule at rest) can avoid some errors physically not acceptable in swarm parameter determination at low $E/N$ such as an electron mean energy lower than gas energy. These kinds of nonphysical Monte Carlo results must also be avoided or minimized because electron swarm data can be used either as input data in fluid equations for discharge modeling or in methods for fitting electron-molecule collision cross sections by unfolding swarm parameters.

At low $E/N$, there is another problem which can appear in the case of highly electronegative gases such as $SF_6$. The strong electron attachment occurring at low energy (lower than 0.5 eV for $SF_6^-$ ion formation by electron impact) can absorb enough initial seed electrons to stop Monte Carlo code.

The purpose of this paper is to present a Monte Carlo method available whatever $E/N$, but which is more adapted for low $E/N$ values (from 0 Td up to some tens of Td). In this method, described in Sec. II, the energy exchanged between electrons and molecules during elastic, inelastic, and superelastic impacts is properly taken into account. Then, the cross sections used and the analysis of corresponding results, showing the validity of the present methods at low $E/N$, are given in Sec. III in the case of electropositive (He) and slightly electronegative gases ($H_2O$). Finally, in the particular case of a strongly electronegative gas ($SF_6$), electron swarm parameters are calculated using an improved Monte Carlo method based on an additional fictitious ionization process in order to avoid the problem of the vanishing of seed electrons due to the high electron attachment

 

efficiency in $SF_6$ at low $E/N$. It is to be noted that a symmetric idea (based on fictitious attachment process) was already applied to $N_2$ at high $E/N$ strength by Li, Pitchford, and Moratz [1] in order to reduce the number of simulated electrons and therefore the computing time.

## II. MONTE CARLO METHOD

The electron transport in a gas under the influence of an electric field $E$ can be simulated with the help of a Monte Carlo method from an initially great number of seed electrons. These primary electrons are treated one by one from their creation until their disappearance out of the domain of the simulation or by specific collisional processes (e.g., attachment). Every electron, during its transit in the gas, performs a succession of free flights punctuated by elastic, inelastic, or superelastic collisions with molecules of gas defined by collision cross sections. During the successive collisions for every electron, certain information (velocity, position, etc.) is stored in order to calculate, from appropriate sampling methods, distribution functions and transport coefficients. The simulation is stopped when all the primary electrons as well as the secondary electrons (created, for example, by ionization) are treated.

The flow chart of Monte Carlo method described hereafter is shown in Fig. 1. As it can be seen, after definitions of the simulation parameters, the gas, and the initial conditions, it is necessary to know first the time of free flight.

### A. Time of free flight $t_{\text{flight}}$

The time of free flight is calculated by using the null collision method initially developed by Skullerud [2] for simulation of ion motion in gases and then used by numerous authors [3]:

$$t_{\text{flight}} = -\frac{\ln(r_{\text{flight}})}{\nu_{\text{tot}}} , \tag{1}$$

where $r_{\text{flight}}$ is a random number uniformly distributed in the [0,1] range and $\nu_{\text{tot}}$ is the total collision frequency including total electron-molecule collision frequency $\nu$ and a null collision frequency $\nu_{\text{null}}$ chosen in order to have always $\nu_{\text{tot}}$ constant:

$$\nu_{\text{tot}} = \nu + \nu_{\text{null}} = \text{const} . \tag{2}$$

### B. Trajectory between two successive collisions

The trajectory between two successive collisions is obtained from the classical mechanic equations. In the framework of this paper, the electric field accelerating electrons (with charge $-e$, mass $m$, position $\mathbf{r}$, and velocity $\boldsymbol{v}$) is assumed to be antiparallel to the $z$ axis. Under these conditions, the components $v_{x1}$, $v_{y1}$, and $v_{z1}$ in the laboratory frame of velocity $\mathbf{v}_1(t_1)$ at time $t_1$ at the end of the free flight can be written as a function of velocity $\boldsymbol{v}_0(t_0)$ (at initial time $t_0$ and with components $v_{x0}$, $v_{y0}$, and $v_{z0}$ in the laboratory frame). Then, new coordinates $\mathbf{r}_1(x_1,y_1,z_1)$ of electron at time $t_1$ can be calculated from coordinates $\mathbf{r}_0(x_0,y_0,z_0)$ of an electron at time $t_0$:

$$\begin{aligned} x_1 &= x_0 + v_{x0} t_{\text{flight}} , \\ y_1 &= y_0 + v_{y0} t_{\text{flight}} , \\ z_1 &= z_0 + v_{z0} t_{\text{flight}} + \frac{1}{2}\frac{eE_z}{m} t_{\text{flight}}^2 , \end{aligned} \tag{3}$$

with $t_{\text{flight}} = t_1 - t_0$.

So, starting from the electron parameters $t_0, \boldsymbol{v}_0, \mathbf{r}_0$ at the beginning of the free flight, the new electron parameters $t_1, \boldsymbol{v}_1, \mathbf{r}_1$ at the end of the free flight are obtained, respectively, from relations (1) and classical mechanic equations. Then just after collision occurring at time $t_1$, electron parameters become $t_1', \boldsymbol{v}_1', \mathbf{r}_1'$. However, it is

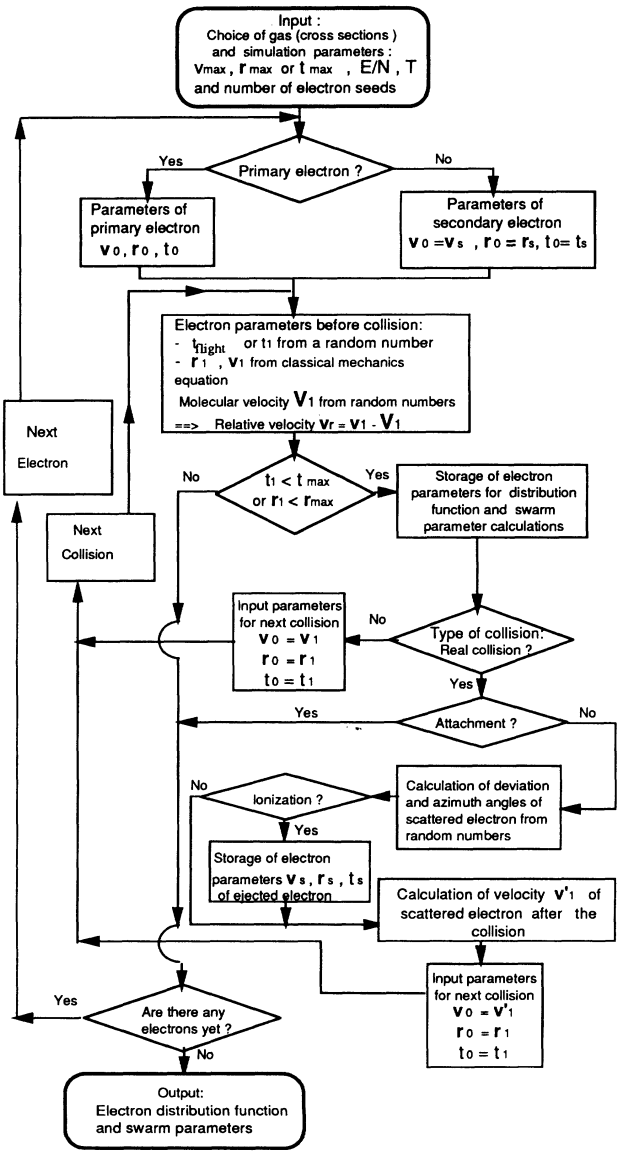


FIG. 1. Flow chart for Monte Carlo simulation of electron swarm motion in a gas under action of an accelerating electric field $E$ (velocity $v_{\max}$, position $r_{\max}$, and time $t_{\max}$ correspond to the possible limits of the simulation domain: see Sec. II for an explanation of the other notations used).

necessary to calculate only electron velocity $\boldsymbol{\nu}_1'$ because the electron-molecule interaction is assumed to be instantaneous ($t_1'=t_1$) and local ($\mathbf{r}_1'=\mathbf{r}_1$). In order to calculate the velocity $\boldsymbol{\nu}_1'$, it is necessary to know the collision type.

### C. Type of collision

The collision type necessitates knowledge of the likelihoods ($p_{\mathrm{col,el}}$, $p_{\mathrm{col,in}}$, $p_{\mathrm{col,sup}}$, or $p_{\mathrm{col,null}}$) of the occurrence of every collision kind (elastic, inelastic, superelastic, or null):

$$p_{\mathrm{col,el}}=\frac{\nu_{\mathrm{el}}}{\nu_{\mathrm{tot}}},\quad p_{\mathrm{col,in}}=\frac{\nu_{\mathrm{in}}}{\nu_{\mathrm{tot}}},$$
$$p_{\mathrm{col,sup}}=\frac{\nu_{\mathrm{sup}}}{\nu_{\mathrm{tot}}},\quad p_{\mathrm{col,null}}=\frac{\nu_{\mathrm{null}}}{\nu_{\mathrm{tot}}} \tag{4}$$

with

$$p_{\mathrm{col,el}}+p_{\mathrm{col,in}}+p_{\mathrm{col,sup}}+p_{\mathrm{col,null}}=1 .$$

In fact, collision frequencies for the different processes ($\nu_{\mathrm{el}},\nu_{\mathrm{in}},\nu_{\mathrm{sup}}$) depend on the relative velocity $\nu_r$ before the collision, which is defined as $\nu_r=|\boldsymbol{\nu}_1-\mathbf{V}_1|$; $\mathbf{V}_1$ is the known velocity of target molecule having a Maxwellian distribution.

The collision type is then determined from a random number $r_{\mathrm{col}}$ uniformly distributed between 0 and 1. Several types of collision are possible: (i) if it is a null collision, velocities before and after the collision are the same; (ii) if it is, for instance, an attachment, the next primary electron is treated; and (iii) if it is another real collision, the velocity $\boldsymbol{\nu}_1'$ after interaction depends on the collision type; the components of electron velocity $\boldsymbol{\nu}_1'$ are given hereafter.

### D. Velocity $\boldsymbol{\nu}_1'$ after a real collision

Let $m$ and $M$ be electron and molecule masses, $\boldsymbol{\nu}_1$ and $\mathbf{V}_1$ their respective velocities in the laboratory frame before the collision, and $\boldsymbol{\nu}_1'$ and $\mathbf{V}_1'$ after the collision. Unknown velocities $\boldsymbol{\nu}_1'$ and $\mathbf{V}_1'$ can therefore be determined from the classical conservation equation of momentum transfer, yielding

$$\boldsymbol{\nu}_1'=\frac{M}{m+M}\boldsymbol{\nu}_r'+\frac{m\boldsymbol{\nu}_1+M\mathbf{V}_1}{m+M} , \tag{5a}$$

$$\mathbf{V}_1'=-\frac{m}{m+M}\boldsymbol{\nu}_r'+\frac{m\boldsymbol{\nu}_1+M\mathbf{V}_1}{m+M} . \tag{5b}$$

Of the right-hand term of relations (5), only the velocity $(m\boldsymbol{\nu}_1+M\mathbf{V}_1)/(m+M)$ of the center-of-mass frame is already known. The unknown vector $\boldsymbol{\nu}_r'$ ($\boldsymbol{\nu}_r'=\boldsymbol{\nu}_1'-\mathbf{V}_1'$) represents the relative velocity after the collision. The modulus $\nu_r'$ and the direction of vector $\boldsymbol{\nu}_r'$ are given hereafter.

The relative speed $\nu_r'$, which is obtained from the classical conservation equation of total energy, depends on collision type. For an elastic collision

$$\nu_r'=\nu_r . \tag{6a}$$

For an excitation of rotational, vibrational, or optical level from the lower level $i$ with potential energy $\varepsilon_i$ to the upper level $j$ with energy $\varepsilon_j$

$$\nu_r'=\left[\nu_r^2-\frac{2}{\mu_r}\Delta\varepsilon_{ji}\right]^{1/2} . \tag{6b}$$

For a superelastic processes corresponding to deexcitation from the upper level $j$ with potential energy $\varepsilon_j$ to the lower level $i$ with energy $\varepsilon_i$

$$\nu_r'=\left[\nu_r^2+\frac{2}{\mu_r}\Delta\varepsilon_{ji}\right]^{1/2} . \tag{6c}$$

$\mu_r$ is the reduced mass: $\mu_r=mM/(m+M)$, and $\Delta\varepsilon_{ji}=\varepsilon_j-\varepsilon_i$.

Then the knowledge of the scattering angle $\chi$ and the azimuthal angle $\eta$ can give the direction of the vector $\boldsymbol{\nu}_r'$ in the center-of-mass frame. The deflection angle $\chi$, between the relative velocity $\boldsymbol{\nu}_r$ before and $\boldsymbol{\nu}_r'$ after a collision, varies between 0 and $\pi$. It depends on the differential cross section $\sigma(\nu,\chi)$ and is determined from a uniform random number $r_\chi$ belonging to the [0,1] range:

$$r_\chi=\frac{\int_0^\chi\sigma(\nu,\chi')\sin\chi'd\chi'}{\int_0^\pi\sigma(\nu,\chi')\sin\chi'd\chi'} . \tag{7a}$$

When an isotropic scattering is assumed, this relation becomes $\cos\chi=1-2r_\chi$. The azimuthal angle $\eta$ can be also assumed to be uniformly distributed in the $[0,2\pi]$ range and is calculated from a uniform random number $r_\eta$:

$$\eta=2\pi r_\eta . \tag{7b}$$

So, as the relative speed $\nu_r'$ is determined from relations (6) of the conservation of total energy and the $\chi$ and $\eta$ angles from relations (7), the vector $\boldsymbol{\nu}_r'$ is therefore completely defined in the center-of-mass frame. But in relations (5), the vector $\boldsymbol{\nu}_r'$ is needed in the laboratory frame; such a transformation is undertaken using the classical Euler relations

$$\nu_{rx}'=\nu_r'(-\sin\chi\sin\eta\sin\phi_r+\sin\chi\cos\eta\cos\theta_r\cos\phi_r+\cos\chi\sin\theta_r\cos\phi_r) ,$$
$$\nu_{ry}'=\nu_r'(\sin\chi\sin\eta\cos\phi_r+\sin\chi\cos\eta\cos\theta_r\sin\phi_r+\cos\chi\sin\theta_r\sin\phi_r) ,$$
$$\nu_{rz}'=\nu_r'(-\sin\chi\cos\eta\sin\theta_r+\cos\chi\cos\theta_r) ,$$

where $\theta_r$ is the polar angle and $\phi_r$ the azimuthal angle in the laboratory frame of vector $\boldsymbol{\nu}_r$. Then, from relation (5a), it is possible to calculate electron velocity $\boldsymbol{\nu}_1'$ in the laboratory frame without neglecting, as usual the velocity $\mathbf{V}_1$ of target molecule; the vector $\mathbf{V}_1$ is of course completely defined because the distribution of background molecular gas is a known Maxwellian. Noting that if the target molecule is considered to be at rest ($\mathbf{V}_1=0$) and $m$ negligible in comparison to $M$ (i.e., $m+M\cong M$), relations (5a) and (6) reduce to the classical relations usually used in the literature for collision treatment in Monte Carlo method.

Concerning ionization processes, the previous relation (6b) used for excitation processes is still valid, but is not necessary. The reason is that ionization processes involve generally an energy amount much higher than the energy gas, so that the assumption of a background molecule at rest can be considered as a good approximation. Following this approximation, the residual energy, after a simple ionization process with threshold $\varepsilon_{\text{ion}}$, is shared between scattered ($\varepsilon_1'$) and ejected ($\varepsilon_{ej}$) electrons following the relation $\varepsilon_1'+\varepsilon_{ej}=\frac{1}{2}m\nu_1^2-\varepsilon_{\text{ion}}$. The energy sharing depends on the knowledge of the differential ionization cross section $\sigma_{\text{ion}}(\varepsilon_1,\varepsilon)$. As ejected and scattered electrons are not discernable, the energy of one of the two electrons ($\varepsilon_{ej}$, for instance) can be obtained from a uniform random number $r_{\text{ion}}$ from

$$r_{\text{ion}}=\frac{\int_0^{\varepsilon_{ej}}\sigma_{\text{ion}}(\varepsilon_1,\varepsilon)d\varepsilon}{\sigma_{\text{ion}}(\varepsilon_1)} ,$$

where $\sigma_{\text{ion}}(\varepsilon_1)$ is the integral ionization cross section and $\varepsilon_1$ the incident energy ($\varepsilon_1=\frac{1}{2}m\nu_1^2$). The scattered electron, after an ionizing collision, is then deflected following an angle $\chi$, assumed to be isotropic, and the ejected electron is deflected following an angle $\chi'$, assumed to be orthogonal to the $\chi$ direction ($\chi'=\chi+\pi/2$). Previous relations give the components of the velocity vectors of scattered $\boldsymbol{\nu}_1'$ ($\nu_1',\chi,\eta$) and ejected $\boldsymbol{\nu}_{ej}(\nu_{ej},\chi',\eta)$ electrons in the center-of-mass frame. The corresponding components in the laboratory frame are then determined using the classical Euler transformation, which can be written in the case of, for example, the scattered electron with velocity $\boldsymbol{\nu}_1'$.

$$\begin{aligned}
\nu_{x1}'&=\nu_1'(-\sin\chi\sin\eta\sin\phi_1+\sin\chi\cos\eta\cos\theta_1\cos\phi_1\\
&\quad+\cos\chi\sin\theta_1\cos\phi_1) ,\\
\nu_{y1}'&=\nu_1'(\sin\chi\sin\eta\cos\phi_1+\sin\chi\cos\eta\cos\theta_1\sin\phi_1\\
&\quad+\cos\chi\sin\theta_1\sin\phi_1) ,\\
\nu_{z1}'&=\nu_1'(-\sin\chi\cos\eta\sin\theta_1+\cos\chi\cos\theta_1) ,
\end{aligned}$$

where $\theta_1$ is the polar angle and $\phi_1$ the azimuthal angle in the laboratory frame of the incident vector $\boldsymbol{\nu}_1$.

### E. Distribution functions and transport coefficients

From previous relations, it is possible to calculate electron parameters $t$, $\boldsymbol{\nu}$, and $\mathbf{r}$ for every collision. These then enable the determination of electron distribution functions and transport coefficients (swarm parameters and reaction rates) from an appropriate sampling method.

In the case considered in this paper of an electric field antiparallel to $z$ axis, the electron distribution function $f(t,\boldsymbol{\nu},z)$ can be decomposed (due to the symmetry revolution around the $z$ axis) in series of polynomial Legendre $P_l(\cos\theta)$, where $\theta$ is the angle between electron velocity $\boldsymbol{\nu}$ and direction of electric field acceleration:

$$f(t,\boldsymbol{\nu},z)=\sum_0^{\infty}\phi_l(t,\nu,z)P_l(\cos\theta) , \tag{8}$$

$\phi_l(t,\nu,z)$, representing the isotropic part ($l=0$) and successive anisotropies ($l>0$) of the distribution function $f(t,\nu,z)$, is directly obtained from a Monte Carlo simulation similarly to Penetrante, Bardsley, and Pitchford [4]. In other words, the energy $\varepsilon$ domain $[0,\varepsilon_{\max}]$, where $\varepsilon$ is the electron incident energy ($\varepsilon=\frac{1}{2}m\nu^2$) and $\varepsilon_{\max}$ its maximum value, is first divided into $n\nu$ regular intervals: $[0,\varepsilon_{\max}]=[\varepsilon_0=0,\varepsilon_1,\ldots,\varepsilon_{k-1},\varepsilon_k,\varepsilon_{k+1},\ldots,\varepsilon_{n\nu}=\varepsilon_{\max}]$ with constant energy step $\Delta\varepsilon=\varepsilon_{k+1}-\varepsilon_k$. Then a discrete function $\Phi_l(t,\varepsilon_{k+1/2},z)$ is defined such as

$$\Phi_l(t,\varepsilon_{k+1/2},z)=\sum_{j=1}^{n_j}\sum_{i=1}^{n_i}\delta(\varepsilon_{ij})P_l(\cos\theta_{ij}) , \tag{9}$$

with $\delta(\varepsilon_{ij})=1$ if $\varepsilon_k<\varepsilon_{ij}<\varepsilon_{k+1}$ and $\delta(\varepsilon_{ij})=0$ elsewhere; the indices $i$ and $j$ correspond to electron number $j$ just before undergoing collision number $i$. $n_i$ is the collision number per electron at time $t$ and in the plane $z$ and $n_j$ the number of corresponding electrons. The isotropic part $\phi_0(t,\varepsilon,z)$ of the distribution function and anisotropy $\phi_l(t,\nu,z)$ of order $l$ can then be obtained from the following relation [4]:

$$\phi_l(t,\varepsilon_{k+1/2},z)=\frac{2l+1}{\sqrt{\varepsilon_{k+1/2}}}\frac{\Phi_l(t,\varepsilon_{k+1/2},z)}{n_e(t,z)} , \tag{10}$$

where $n_e(t,z)$ is the electron number density used as normalization quantity for the distribution function $\phi_l(t,\varepsilon_{k+1/2},z)$.

Concerning transport coefficients such as drift velocity $W$, longitudinal $D_L$ or transverse $D_T$ diffusion coefficients, mean energy $\langle\varepsilon\rangle$, ionization $\langle\nu_{\text{ion}}\rangle$ or attachment frequency $\langle\nu_{\text{att}}\rangle$, etc., they are then calculated using a statistical mean based on conventional formulas. For instance, the time evolution of transport coefficients is obtained by first discretizing the time domain $[0,t_{\max}]$ in $nt$ regular intervals: $[0,t_{\max}]=[t_0=0,\ t_1,\ldots,t_{m-1},\ t_m,\ t_{m+1},\ldots,t_{nt}=t_{\max}]$ with constant time step $\Delta t=t_{m+1}-t_m$.

Then the relations for transport coefficients such as $\langle\varepsilon\rangle$, $W$, $\langle\nu_{\text{ion}}\rangle$, or $\langle\nu_{\text{att}}\rangle$ can have the following form in each time step ($t_{m+1}-t_m$):

$$\langle\varepsilon\rangle_{m+1/2}=\frac{1}{n_{j,m+1/2}}\sum_{j=1}^{n_{j,m+1/2}}\frac{1}{n_{i,m+1/2}}\sum_{i=1}^{n_{i,m+1/2}}\varepsilon_{ij,m+1/2} , \tag{11a}$$

$$W_{m+1/2}=\frac{1}{n_{j,m+1/2}}\sum_{j=1}^{n_{j,m+1/2}}\frac{1}{n_{i,m+1/2}}\sum_{i=1}^{n_{i,m+1/2}}\nu_{z,ij,m+1/2} , \tag{11b}$$

$$\langle\nu_{\text{ion or att}}\rangle_{m+1/2}=\upsilon_{\text{tot}}\frac{1}{n_{j,m+1/2}}\times\sum_{j=1}^{n_{j,m+1/2}}\frac{1}{n_{i,m+1/2}}\sum_{i=1}^{n_{i,m+1/2}}n_{\text{ion or att},ij,m+1/2} . \tag{11c}$$

$\varepsilon_{ij,m+1/2}$ and $v_{z,ij,m+1/2}$ correspond to the kinetic energy and the velocity component along the $z$ axis of electron number $j$ undergoing collision number $i$ in the interval $[t_m,t_{m+1}]$, while $n_{\text{ion},ij,m+1/2}$ (or $n_{\text{att},ij,m+1/2}$) is the number of ionizations (or attachments) per electron in the same time interval and total collision frequency $v_{\text{tot}}$ is already defined in relation (2). $n_{j,m+1/2}$ represents the electron number counted in the time interval $[t_m,t_{m+1}]$ and $n_{i,m+1/2}$ the number of collisions undergone by electron $j$ in the same time interval.

Previous relations (11) give the time dependence of macroscopic coefficients, while their space dependence, along the $z$ axis, for example, can be obtained by discretizing the space domain $[0,z_{\max}]$ in $nz$ regular intervals: $[0,z_{\max}]=[z_0=0,z_1,\ldots,z_{s-1},z_s,z_{s+1},\ldots,z_{nz}=z_{\max}]$ with constant space step $\Delta z=z_{s+1}-z_s$. Then space variation of, for example, mean energy $\langle\varepsilon\rangle_{s+1/2}$ in each space step $z_{s+1}-z_s$ is obtained from

$$\langle\varepsilon\rangle_{s+1/2}=\frac{1}{n_{j,s+1/2}}\sum_{j=1}^{n_{j,s+1/2}}\frac{1}{n_{i,s+1/2}}\sum_{i=1}^{n_{i,s+1/2}}\varepsilon_{ij,s+1/2}\ , \tag{12}$$

where $\varepsilon_{ij,s+1/2}$ is the kinetic energy for an electron number $j$ undergoing collision number $i$ in the space interval $[z_s,z_{s+1}]$, while $n_{j,s+1/2}$ represents the electron number counted in the interval $[z_s,z_{s+1}]$ and $n_{i,s+1/2}$ the collision number undergone by the electron $j$ in the same space interval.

## III. RESULTS AND DISCUSSIONS

In Secs. III A and III B, calculations of distribution functions and transport coefficients are carried out in molecular gases ($H_2O$) and atomic gas (He) chosen in order to check first the validity of the present Monte Carlo method and then to give insight into electron swarm data in the case of dominant low $E/N$ collisional processes (i.e., thermal motion of target, inelastic, and superelastic collisions). Section III C is devoted to the case of strongly attaching gases.

The set of electron-He cross sections is taken from the literature (see, e.g., [5]). Collision cross sections chosen for $H_2O$ are already partly fitted elsewhere [6] by comparing measured and calculated transport coefficients using a multiterm Boltzmann equation solution [8]. This set of electron-$H_2O$ cross sections includes elastic momentum transfer, excitations of ten rotational, two vibrational, and nine optical levels, and also ionization and attachment processes. Each electron-molecule collision cross section $\sigma_{ji}(\varepsilon)$ for deexcitation (superelastic processes) through the upper level $j$ to the allowed lower level $i$ is determined from the excitation cross section $\sigma_{ij}(\varepsilon)$ by using the well known principle of detailed balance (see, e.g., [9]):

$$\sigma_{ji}(\varepsilon)=\frac{g_i}{g_j}\frac{\varepsilon+\Delta\varepsilon_{ij}}{\varepsilon}\sigma_{ij}(\varepsilon+\Delta\varepsilon_{ij})\ ,$$

where $g_i$ and $g_j$ denote the statistical weight of the levels $i$ and $j$, respectively [$\Delta\varepsilon_{ij}$ is already defined in relations (6)].

### A. Zero-field electron swarm results

Probably one of the most convincing validity tests of the treatment of low energy electron-molecule collisions with the Monte Carlo method is to determine distribution functions and transport coefficients under zero-field conditions. Indeed, for an electron swarm or beam released (with known initial energetic and angular distributions) through a gas under zero-electric field conditions, it is well established that this electron swarm relaxes after a greater or lesser period of time (depending on initial conditions and background gas) towards an equilibrium distribution, whatever the initial distribution or the nature of the background gas [10]. Such an equilibrium is obviously characterized by a classical behavior: the electron distribution function becomes Maxwellian at the background gas temperature, there is no more electron drift, and diffusion becomes completely isotropic (i.e., longitudinal and transverse diffusion coefficients are identical).

Such a behavior is perfectly illustrated in Figs. 2(a) and 2(b) showing electron mean energy, drift velocity, and also longitudinal and transverse diffusion coefficients in the case of an energetic electron swarm released in $H_2O$ background gas. Figure 2(a), showing an electron mean energy which relaxes towards gas energy whatever the initial electron energy (lower or higher than gas energy), corresponds to a long time scale. In Fig. 2(b), corresponding to shorter time scale, electrons emitted along the forward direction, after a relatively few collisions, lose their initial anisotropic angular distribution so that the initial directed velocity becomes rapidly negligible. In this short time scale, the longitudinal diffusion coefficient, after an overshoot effect due to the anisotropy of the initial distribution, tends towards transverse diffusion. Figure 3 shows another validity test corresponding to the zero-field electron mean energy in He calculated with and without including the thermal motion of background gas. Figure 3 clearly illustrates the consequence for assuming a target at rest since the electron mean energy tends towards zero energy instead of to gas energy (i.e., $\frac{3}{2}kT$). These results, completed with further validity tests not reported in this paper and undertaken in other gases, give us a good reliability concerning the Monte Carlo method described in Sec. II for the treatment of low energy collision processes (energy exchange during elastic, inelastic, and superelastic collisions).

### B. Low $E/N$ electron swarm results

Figures 4(a) and 4(b) show the electron mean energy $\langle\varepsilon\rangle$ and drift velocity $W$ as a function position $z$ along the direction of the electric field acceleration in the case of two relatively low $E/N$ values [31 and 93 Td ($10^{-17}$ V cm$^2$)] background gas. Such Monte Carlo calculations, which can correspond to the simulation of the classical steady-state Townsend experiment (see, e.g., [8]) are undertaken with and without including the effects of superelastic collisions in order to emphasize the influence of these low energy processes on electron transport. So, starting from the cathode ($z=0$) with an initial mono-

kinetic energy (0.038 eV) along the forward direction, electrons are accelerated by the electric field and undergo collisions with the background gas at the same time. Then, after a certain interelectrode distance, where an equilibrium between collisions and electric field can be (or not) reached depending on discharge conditions, electrons arrive at the anode (assumed to be completely absorbing), which breaks down the eventual equilibrium phase.

For $E/N=31$ Td [Fig. 4(a)], after a short nonequilibrium distance near the cathode, $W$ and $\langle\varepsilon\rangle$ reach their equilibrium values, which are not the same, according to whether superelastic collisions are considered or not. Naturally, when superelastic collisions are not included in Monte Carlo simulation, the mean energy values are not realistic (lower than gas energy) and the drift velocity is overestimated because, as is known, superelastic collisions which increase the total frequency collision lead to a more isotropic electron swarm and therefore to a lower drift velocity. For $E/N=93$ Td [Fig. 4(b)], electron transport cannot really reach an equilibrium regime since more particularly the mean energy continually increases from the cathode until the anode; however, this slope, which is perturbed by the electrode effect, increases faster near the anode. This is due to the gap distance (0.5 cm for 1 Torr gas pressure) chosen not large enough to enable an equilibrium regime for electron mean energy. However, the drift velocity, which has a momentum exchange time shorter than its energy exchange time (e.g., Kunhardt, Wu, and Penetrante [11]) reaches an equilibrium value during a short distance (from about 0.2 up to 0.35 cm) before being perturbed by the presence of the anode. In these cases, the influence of superelastic collision is also not negligible.

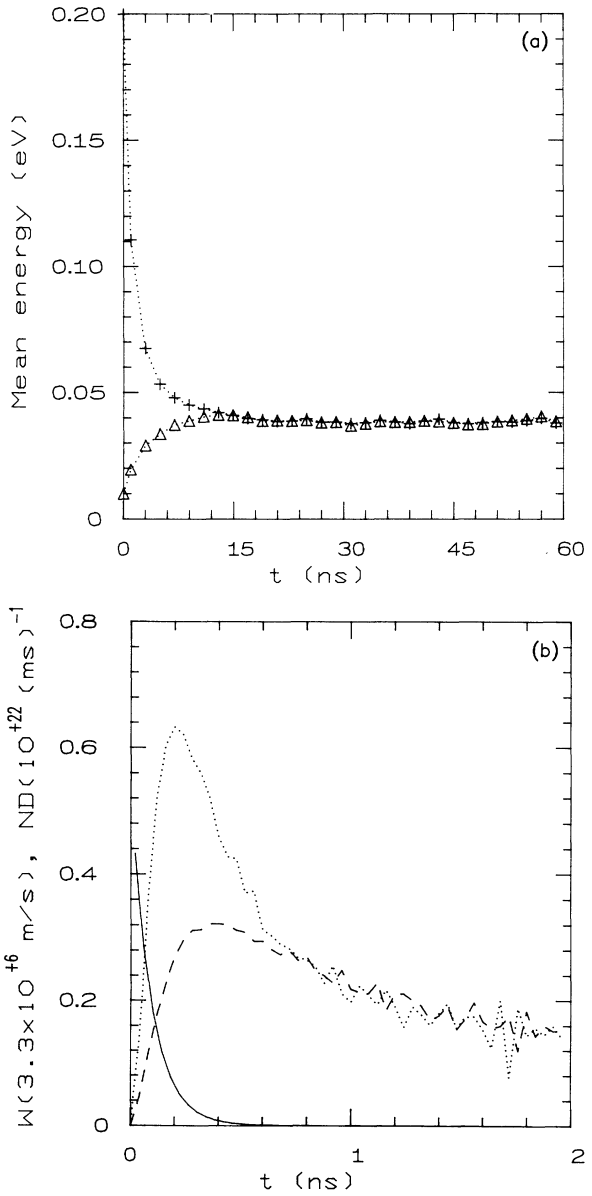


FIG. 2. (a) Zero-field electron mean energy in $H_2O$ for $p=1$ Torr and $T=300$ K in the case of two initial electron beam energies $\varepsilon_0$ distributed along the forward direction: $(..\Delta..\Delta...)$ $\varepsilon_0=0.01$ eV and $(..+..+...)$ $\varepsilon_0=0.2$ eV. (b) Zero-field directed velocity $W(---)$ and longitudinal $ND_L$ $(\cdot\cdot\cdot\cdot)$ and transverse $ND_T$ $(---)$ diffusion coefficients in $H_2O$ for $p=1$ Torr, $T=300$ K, and an initial electron beam with energy $\varepsilon_0=0.2$ eV distributed along the forward direction.

Figure 5 shows longitudinal $D_L/\mu$ ($\mu$ is electron mobility) and transversal $D_T/\mu$ characteristic energies in $H_2O$ as a function of $E/N$. $D_L/\mu$ and $D_T/\mu$ values are obtained in the case of an unbounded system (i.e., electrons are assumed quite far from electrodes and sources) when the memory of the initial conditions of electrons is lost. This means that these Monte Carlo calculations correspond to the simulation of the classical time of flight experiment (see, e.g. [8]), which give us the usual hydrodynamic swarm parameters such as drift velocity, diffusion coefficients, and reaction rates. In Fig. 5, the

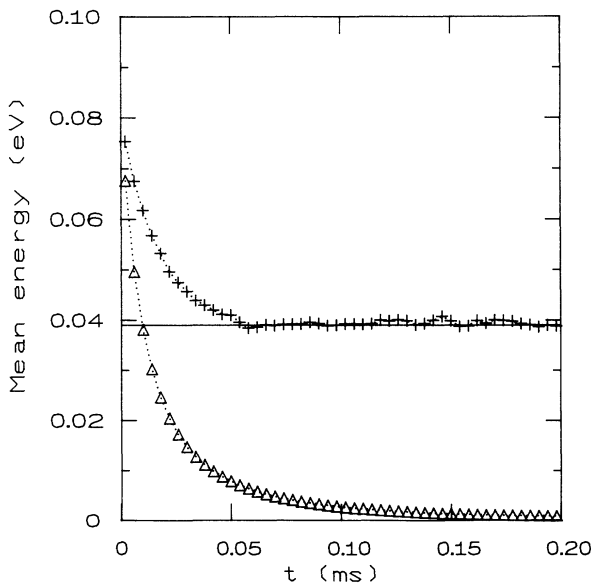


FIG. 3. Zero-field electron mean energy in He for $p=1$ Torr, $T=300$ K, and an initial electron beam energy $\varepsilon_0=0.1$ eV distributed along forward direction: $(..+..+...)$ including thermal motion of targets and $(..\Delta...\Delta...)$ target assumed to be at rest.

$D_L/\mu$ and $D_T/\mu$ data, calculated from two different sets of $H_2O$ cross sections (Yousfi and co-workers [6] and Hayashi [7]), are compared to measurements (Ref. [12] for $D_L/\mu$ and Ref. [13] for $D_T/\mu$). It should be known that the main differences between the two cross section sets are situated in the low kinetic energy range:

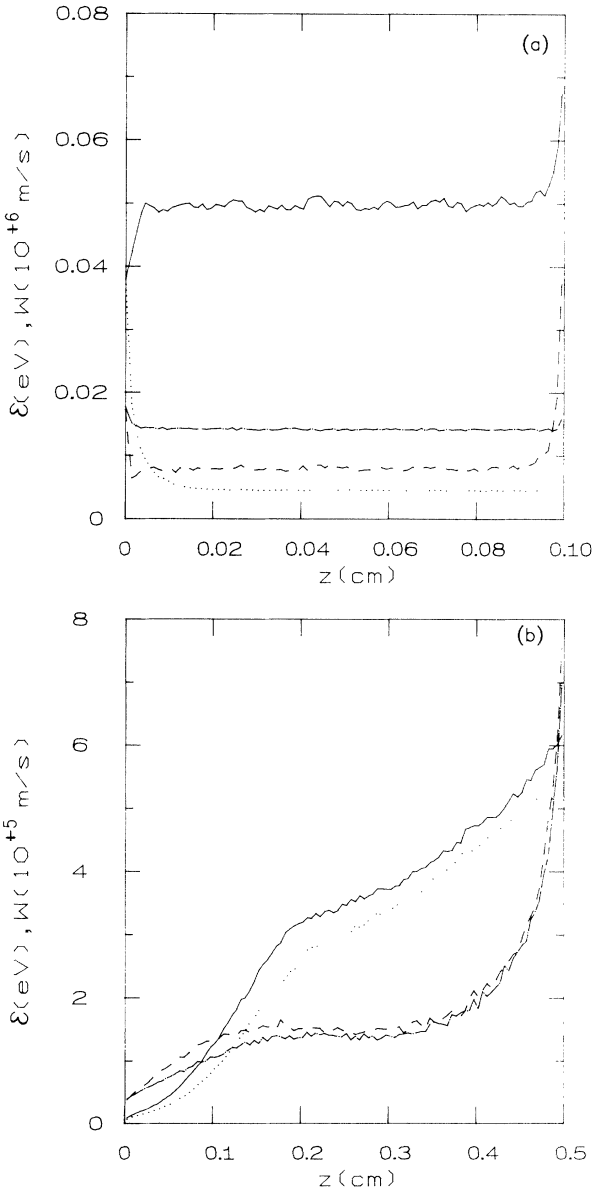


FIG. 4. (a) Variation between cathode ($z=0$) and anode ($z=0.1$ cm) of electron mean energy (—— and · · · ·) and drift velocity (— — — and –.–) in $H_2O$ for $p=1$ Torr, $T=300$ K, $V_a=1$ V, and an initial low energy electron beam ($\varepsilon_0=0.038$ eV) emitted at the cathode along the forward direction with and without including superelastic collisions: with (——), (— — —) and without (· · · ·), (–.–). (b) Variation between cathode ($z=0$) and anode ($z=0.5$ cm) of electron mean energy (—— and ...) and drift velocity (— — — and –.–) in $H_2O$ for $p=1$ Torr, $T=300$ K, $V_a=5$ V, and an initial low energy beam $\varepsilon_0=0.038$ eV) emitted at the cathode along the forward direction with and without including superelastic collisions: with (——), (— — —) and without (· · · ·), (–.–).

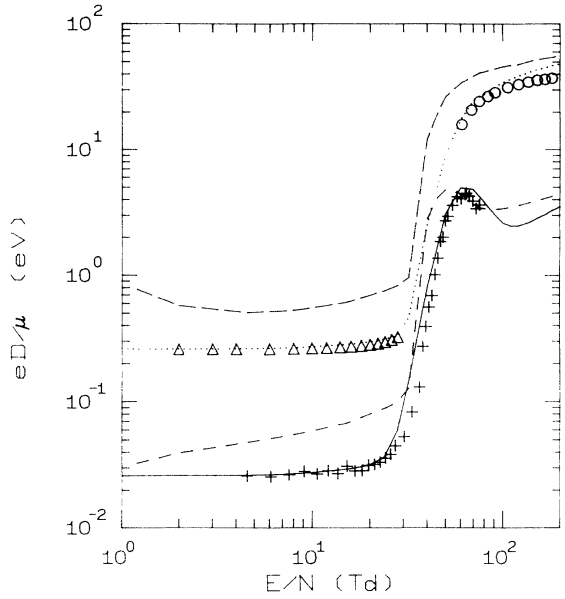


FIG. 5. Hydrodynamic values of longitudinal $eD_L/\mu$ (++, — — —; and ——) and transverse $eD_T/\mu$ (ΔΔ; ○ ○; · · ·; and — — —) characteristic energies in $H_2O$ for $T=294$ K. Symbols: measurements (+, Wilson *et al.* [12]; Δ and ○, Elford and co-workers [13]). Lines: Monte Carlo simulations using Yousfi and co-workers [6] cross sections (· · · · and — — —) and Hayashi [7] cross sections (· · · · and — — —) ($eD_T/\mu$ data are multiplied by 10).

Hayashi's set does not include rotational excitation cross sections (i.e., for energy range from about $10^{-3}$ eV up to $10^{-1}$ eV), which are correctly considered in the set of Yousfi and co-workers (see also Ness and Robson [14]). In fact, at the low energy range, classical crossed beam experiments for cross sections measurements are not reliable enough due mainly to the difficulty of maintaining low energy beams. So it is usual in that case to confirm the calculated cross sections (using the Born approximation for $H_2O$ rotational cross sections) by comparing calculated and measured swarm parameters. It is thus easy to observe in Fig. 5 the good agreement between measurements and Monte Carlo calculations using $H_2O$ set of cross sections taken from Yousfi and co-workers [6] and the rather great sensitivity of electron swarm parameters (about 50% of deviation) due to the difference between cross sections at low kinetic energy dominated by rotational excitation, superelastic collisions, and also energy exchange and thermal motion of molecules which are properly considered in present Monte Carlo method.

### C. Low $E/N$ swarm parameters in strongly electronegative gases

It is known that the electron distribution function and swarm parameters are calculated from the Monte Carlo method by following seed electrons from initial conditions until they vanish either by collisions (e.g., attachment) or by passing beyond the limits of the simulation domain (arrival at anode or reaching maximum time allowed for simulation, etc.).

At low $E/N$ values in gases such as $SF_6$ having high attachment cross sections at low energy (for reaction $e+SF_6 \rightarrow SF_6^-$), most seed electrons, after a few free flights, can be attached. In this case, the classical Monte Carlo simulation is not able to calculate hydrodynamic electron swarm parameters with enough precision. This corresponds to the case where electron current measured, for example, using the classical time resolved experiment (see, e.g. [18]), which is too low to be accurate.

At very $E/N$ values, the Monte Carlo simulation can be completely stopped as all seed electrons are attached to $SF_6$. Under the same conditions, there is no arrival of electrons at the anode in swarm experiments. In that case, it is known that swarm experiments are undertaken not in pure $SF_6$ but in gas mixture including a buffer gas (e.g., $N_2$) and a small admixture of $SF_6$.

In this section, an improved Monte Carlo method is proposed (see Yousfi and Hennad [15]) in order to obtain swarm parameters with a better accuracy in the first case (low $E/N$ values). It is based on an additional fictitious ionization process with a constant ionization frequency $\nu_{\text{fic,ion}}$, which artificially increases the number of simulated electrons. Therefore, the total collision frequency $\nu_{\text{tot}}$ defined by relation (2) becomes $\nu_{\text{tot}}=\nu+\nu_{\text{null}}+\nu_{\text{fic,ion}}$ =const. The collision probability of this new fictitious process is $p_{\text{col,fic,ion}}=\nu_{\text{fic,ion}}/\nu_{\text{tot}}$. Then, for every fictitious ionization collision a new electron is created. In that case, the primary (or scattered) and new (or ejected) electrons are not deflected during this fictitious ionization and both keep the velocity of the incident electron. As all electrons (primary or secondary created either by real ionization or fictitious ionization) are treated, the electron distribution, density, and swarm parameters thus obtained are those of the fictitious gas (including the additional ionization process). Therefore, the problem is to calculate the electron swarm data for the real gas. In the case of spatially infinite medium, it is easy to establish a simple relation between the electron distribution function $f_f(\boldsymbol{v},t)$ of the fictitious gas and $f(\boldsymbol{v},t)$ of the real gas:

$$f(\boldsymbol{v},t)=f_f(\boldsymbol{v},t)e^{-\nu_{\text{fic,ion}}t}. \tag{13}$$

A similar relation can be written between electron number density $n_f(t)$ of the fictitious gas and $n(t)$ of the real gas:

$$n(t)=n_f(t)e^{-\nu_{\text{fic,ion}}t}. \tag{14}$$

Therefore, Monte Carlo calculations will be performed in the fictitious gas including the additional ionization process in order to overcome the problem of the extensive vanishing of seed electrons due to the strong attachment processes. This leads to the calculation of the electron distribution function $f_f$ and the density $n_f$ of the fictitious gas. Then the distribution function $f$ and the number density $n$ of the real gas will be deduced using relations (13) and (14).

In the following this improved Monte Carlo method is applied to $SF_6$ at low $E/N$ values. Collision cross sections of $SF_6$ are taken from Phelps and Van Braunt [16] for excitation processes and from Yousfi [17] for the other collision processes (elastic momentum transfer, attachment, vibration, and ionization). Monte Carlo calculations are performed in the case of an unbounded system (i.e., $\partial/\partial \mathbf{r}=0$) for which relations (13) and (14) are valid and which corresponds (when the memory of initial conditions is lost) to the simulation of classical time of flight or time resolved swarm experiments (see, e.g., [8]).

Figure 6 shows the electron drift velocity and the mean energy in $SF_6$ for $E/N=10$ Td [Fig. 6(a)] and 2 Td [Fig. 6(b)] with and without using fictitious ionization. The chosen initial energy distribution is monokinetic along

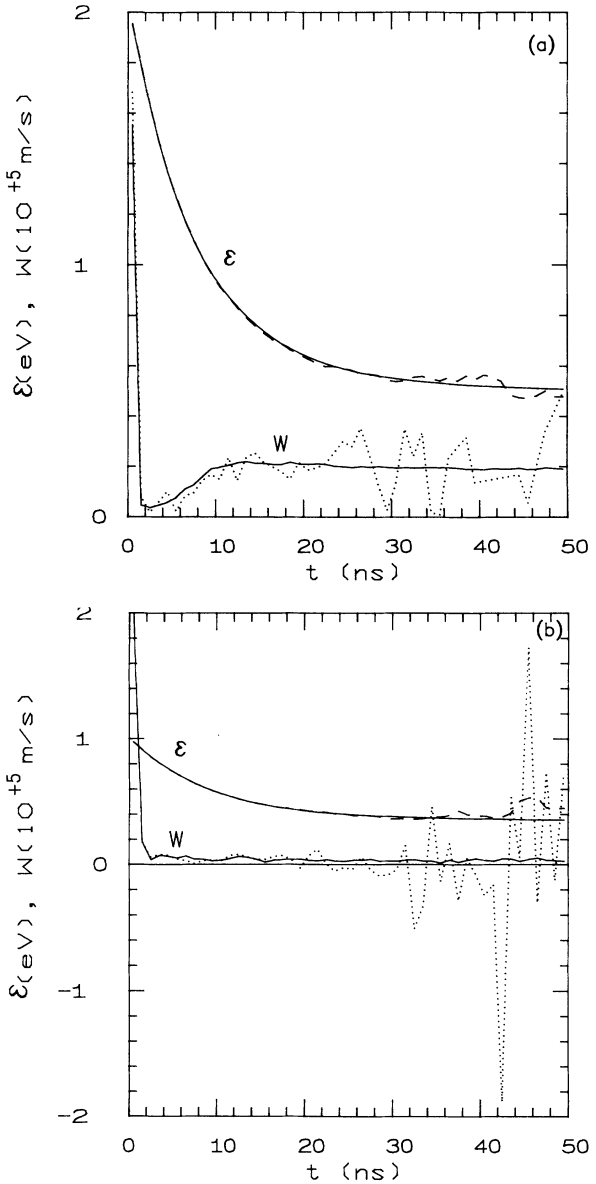


FIG. 6. (a) Electron mean energy (— — —) and drift velocity (· · · ·) in $SF_6$ with (——) and without (— — — and · · · ·) fictitious ionization: $E/N=10$ Td, 5000 seed electrons, initial electron beam with 2 eV emitted along the forward direction and $\nu_{\text{fic,ion}}=2\times10^8\ \text{s}^{-1}$. (b) Electron mean energy (— — —) and drift velocity (· · · ·) in $SF_6$ with (——) and without (— — — and · · · ·) fictitious ionization: $E/N=2$ Td, 10 000 seed electrons, initial electron beam with 1 eV emitted along the forward direction and $\nu_{\text{fic,ion}}=3\times10^8\ \text{s}^{-1}$.

the forward direction and the number of seed electrons considered for the simulation is 5000 for 10 Td and 10 000 for 2 Td. Starting from their initial values, energy and drift velocity relax towards their equilibrium values in both cases (i.e., with and without using fictitious ionization). However, the statistical fluctuations are far from negligible when the fictitious ionization is not used to improve Monte Carlo results. It is to be noted that, due to the large fluctuations, the drift velocity can become negative for a lower $E/N$ value (2 Td) while the improved Monte Carlo method avoids this problem [see Fig. 6(b)]. As expected, statistical fluctuations are more pronounced in the case of the drift velocity, which is a statistical mean only of component $v_z$ of the velocity along the $z$ axis [see relation (11b)], contrary to the mean energy value, which is an average of the square of the three components $v_x$, $v_y$, and $v_z$ [see relation (11(a)]. Thus, for the same number of collisions, the electron mean energy is necessarily more accurate than the drift velocity. Furthermore, the choice of the collision frequency $\nu_{\text{fic,ion}}$ of the fictitious ionization depends on $E/N$ values. As the $E/N$ value decreases, the attachment efficiency in $SF_6$ increases (see, e.g., the time resolved measurements of the attachment coefficients in $SF_6$ of Aschwanden [18]), thus necessitating a larger value of $\nu_{\text{fic,ion}}$ in order to compensate for the vanishing of seed electrons by attachment. For example, the chosen values of $\nu_{\text{fic,ion}}$ are $2\times10^8$ s$^{-1}$ for $E/N=10$ Td and $3\times10^8$ s$^{-1}$ for $E/N=2$ Td.

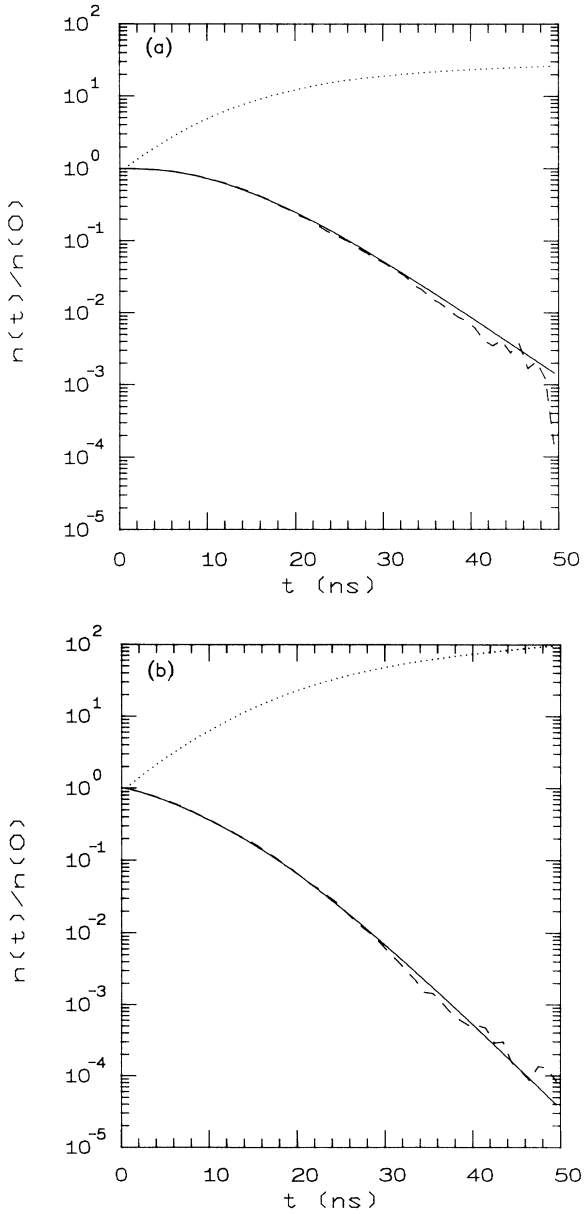


FIG. 7. (a) Reduced electron number density $n(t)/n(0)$ in $SF_6$ with (——) and without (– –) fictitious ionization and also $n_f(t)/n(0)$ (· · · ·): $E/N=10$ Td, 5000 seed electrons, initial electron beam with 2 eV emitted along the forward direction, and $\nu_{\text{fic,ion}}=2\times10^8$ s$^{-1}$. (b) Reduced electron number density $n(t)/n(0)$ in $SF_6$ with (——) and without (– –) fictitious ionization and also $n_f(t)/n(0)$ (· · · ·): $E/N=2$ Td, 10 000 seed electrons, initial electron beam with 1 eV emitted along the forward direction, and $\nu_{\text{fic,ion}}=3\times10^8$ s$^{-1}$.

Figures 7(a) and 7(b) show the electron number densities $n(t)$ and $n_f(t)$ [see relation (14)] in $SF_6$ including the additional fictitious ionization process for $E/N=10$ and 2Td. The electron number density calculated without including fictitious ionization is also shown in these figures. First, the electron number densities calculated with and without using fictitious ionization are, as expected, in good agreement. Concerning the fluctuations, a similar behavior to the swarm parameters shown in Fig. 6 is observed. Indeed, the density calculated with the classical Monte Carlo method shows statistical fluctuations due to the decrease of electron number density. For a lower $E/N$ value [Fig. 7(b)], the decrease of the number density $n(t)$ is more pronounced due to the higher attachment efficiency. Figure 7 also shows the density $n_f(t)$ calculat-

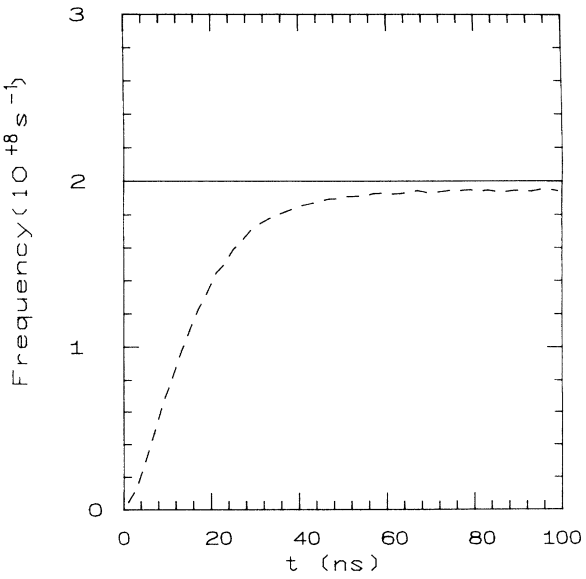


FIG. 8. Electron attachment frequency $\langle \nu_{\text{att}} \rangle$ (— — —) in $SF_6$ with fictitious ionization $\nu_{\text{fic,ion}}=2\times10^8$ s$^{-1}$(——): $E/N=10$ Td, 5000 seed electrons, initial electron beam with 2 eV emitted along the forward direction.

ed with the improved Monte Carlo method using fictitious ionization. In fact, the density $n_f(t)$ varies following the relation $n_f(t)=n(0)e^{(\nu_{\text{fic,ion}}-\langle\nu_{\text{att}}\rangle)t}$, where $\langle\nu_{\text{att}}\rangle$ is the macroscopic attachment frequency of real gas ($SF_6$), already defined in relation (11c).

Therefore, for a given $E/N$ value, it is better to choose a $\nu_{\text{fic,ion}}$ value higher than the attachment frequency $\langle\nu_{\text{att}}\rangle$ to be sure to compensate for electron attachment efficiency. Such a choice is illustrated in Fig. 8, showing the time evolution of the attachment frequency $\langle\nu_{\text{att}}\rangle$ compared to fictitious ionization frequency in $SF_6$ for $E/N=10$ Td. In that case [i.e., $\nu_{\text{fic,ion}}-\langle\nu_{\text{att}}\rangle(t)>0$], the density $n_f(t)$ increases as time evolves, as is shown in Fig. 9. The distribution function $f(\nu,t)$ or the density $n(t)$ [deduced from relation (13) or (14)] and other electron swarm parameters are therefore obtained with better accuracy.

In conclusion, it is to be noted that the present Monte Carlo method is well adapted for the low $E/N$ cases since the dominant collision processes (elastic including energy exchange and thermal motion of gas, inelastic and superelastic) are properly taken into account. This method is also adapted for the cases of strongly electronegative gases such as $SF_6$ by using an additional fictitious ionization process with constant collision frequency.

## ACKNOWLEDGMENTS

The Laboratoire des Decharges Dans Les Gaz is "Unité de Recherche Associée du Centre National de la Recherche Scientifique No. 277."

[1] Y. M. Li, L. C. Pitchford, and T. J. Moratz, Appl. Phys. Lett. **54**, 1403 (1989).

[2] H. R. Skullerud, J. Phys. D **1**, 1567 (1968).

[3] S. L. Lin and J. N. Bardsley, J. Chem. Phys. **66**, 435 (1977); I. D. Reid, Aust. J. Phys. **32**, 231 (1979); J. P. Boeuf and E. Marode, J. Phys. D **15**, 2169 (1982); M. J. Brennan, IEEE Trans. Plasma Sci. **19**, 256 (1991); M. Yousfi, A. Himoudi, and A. Gaouar, Phys. Rev. A **46**, 7889 (1992).

[4] B. M. Penetrante, J. N. Bardsley, and L. C. Pitchford, J. Phys. D **18**, 1087 (1985).

[5] M. Yousfi, G. Zissis, A. Alkaa, and J. J. Damelincourt, Phys. Rev. A **42**, 978 (1990).

[6] G. Friedriech and M. Yousfi, in *XXth International Conference on Phenomena in Ionized Gases, Pisa,* 1991, edited by V. Palleschi and M. Vaselli (Institute of Atomic and Molecular Physics, CNR, Pisa, 1991); M. Yousfi, A. Poinsignon, and A. Hamani, in *Non-Thermal Plasma Technique for Pollution Control,* Vol. 34 of *NATO Advanced Study Institute, Series G: Ecological Sciences,* edited by B. M. Penetrante and S. E. Schultheis (Springer-Verlag, New York, 1993), pp. 299–329.

[7] M. Hayashi, *Swarm Studies an Inelastic Electron-Molecule Collisions,* edited by L. C. Pitchford (Springer-Verlag, New York, 1985), pp. 167–187.

[8] M. Yousfi, P. Segur, and T. Vassiliadis, J. Phys. D **18**, 359 (1985).

[9] L. G. H. Huxley and R. W. Crompton, *The Diffusion and Drift of Electrons in Gases* (Wiley Interscience, New York, 1974).

[10] M. Yousfi and A. Chatwiti, J. Phys. D **20**, 457 (1987).

[11] E. E. Kunhardt, J. Wu, and B. Penetrante, Phys. Rev. A **37**, 1654 (1988).

[12] J. F. Wilson, F. J. Davis, D. R. Nelson, R. N. Compton, and O. H. Crowford, J. Chem. Phys. **62**, 4204 (1975).

[13] R. W. Crompton, M. T. Elford, and R. L. Jory, Aust. J. Phys. **20**, 369 (1967); M. T. Elford, *International Conference on Phenomena in Ionized Gases,* edited by W. T. Williams (University College of Swansea, Swansea, 1987), Vol. 1, pp. 130–131.

[14] K. F. Ness and R. E. Robson, Phys. Rev. A **38**, 1446 (1988).

[15] M. Yousfi and A. Hennad, in *Gaseous Electronic Conference, Montreal 1993,* edited by M. Moisan (University of Montreal, Montreal, 1993).

[16] A. V. Phelps and R. J. Van Braunt, J. Appl. Phys. **64**, 4269 (1989).

[17] M. Yousfi, thèse de Doctorat d'Etat, Université Paul Sabatier de Toulouse, 1986.

[18] Th. Aschwanden, in *Gaseous Dielectrics IV* , edited by L. G. Christophorou (Pergamon, New York, 1984), pp. 24–33.